Turbulence Modeling at High Rotating Rates

Kun Ho Chun, Young Don Whang, Han Young Yoon, Hee Chul Kim, and Sung Quun Zee
KAERI , 150 Deokjin-dong, Yuseong-gu, Daejeon 305-353, ex-khchun@kaeri.re.kr

1. Introduction

Rotating effects in wall-bounded flows appear in many natural and engineering situations. The prediction of the flow in rotating devices and, particularly, the demanding blade cooling technology for industrial and aircraft turbines have motivated many of the existing studies dealing with a rotating channel duct flow. Fluid flow in most of these circumstances is a turbulence flow including a relaminarization region, which is due to high rotating effects. The coupling of the rotation-induced forces on a turbulence structure has been extensively studied in the channel flow and square-cross section duct flow.

2. Turbulence Modeling

The Reynolds stress transport equation with the redistribution tensor proposed by Durbin[1] is written as

$$\frac{D\overline{u_i u_j}}{Dt} = P_{ij} + R_{ij} + D_{ij}^{v} + D_{ij}^{t} + \wp_{ij} - \frac{\overline{u_i u_j}}{k}\varepsilon \qquad (1)$$

and

$$\wp_{ij} = \Pi_{ij} - \varepsilon_{ij} + \frac{\overline{u_i u_j}}{k}\varepsilon \qquad (2)$$

are identified as the generation due to the mean shear (P_{ij}) and system rotation (R_{ij}), viscous diffusion (D_{ij}^{v}) and turbulent diffusion (D_{ij}^{t}) associated with the velocity and redistribution ($\wp_{ij}$), respectively.

The velocity-pressure gradient correlation is

$$\Pi_{ij} = -\frac{1}{\rho}\left(\overline{u_i \frac{\partial p}{\partial x_j}} + \overline{u_j \frac{\partial p}{\partial x_i}}\right), \qquad (3)$$

which is the sum of the pressure-strain correlation Φ_{ij} and pressure diffusion D_{ij}^{p}. Conventionally, they have been separately modeled since the trace (obtained by setting $i = j$ and summing) of Φ_{ij} is zero. It appears more appropriate to composite them in the elliptic relaxation approach, since Π_{ij} not Φ_{ij} balances the difference between the dissipation and molecular diffusion at the wall.

$$f_{ij} - (1 - f_a)\nabla \circ (L^2 \nabla f_{ij}) = \frac{\Phi_{ij}^{h}}{k} + \left(\frac{\overline{u_i u_j}}{k} - \frac{2}{3}\delta_{ij}\right)\frac{1}{T} \qquad (4)$$

The function $(1 - f_a)$ used here is modeled by the second Reynolds stress invariant $A_2 (= a_{ij}a_{ji})$. The redistribution tensor $\wp_{ij} (= kf_{ij})$ is obtained from the solution f_{ij} of the elliptic relaxation equation. The length scale L and time scale T are defined as

$$L = C_L\left(\frac{k^{3/2}}{\varepsilon} + C_\eta\left(\frac{\nu^3}{\varepsilon}\right)^{1/4}\right) \qquad (5)$$

and

$$T = \max\left(\frac{k}{\varepsilon}, C_T\left(\frac{\nu}{\varepsilon}\right)^{1/2}\right). \qquad (6)$$

The boundary conditions of f_{ij} are also applied at the wall: $f_{11} = 0$, $f_{22} = -20\nu^2\overline{u_2 u_2}/\varepsilon y^4$, $f_{33} = 0$, and $f_{12} = -20\nu\overline{u_1 u_2}/\varepsilon y^4$.

3. Results and Discussion

In the simulations for a rotating channel flow due to the elliptic relaxation model, the models of Wizman *et al.* [2] and Pettersson & Andersson[3] were successfully applied to the rotating flow with an additional source term in the dissipation rate transport equation. On the examination for the dissipation rate of an isotropic turbulence, Speziale *et al.* [4] demonstrated that the additional term in the dissipation rate equation is not only theoretically unfounded but also is limited at a local rotation number. The use of the term can induce an unphysical phenomena on industrial applications since the additional term is purely empirical. In the present calculations, the additional source term in the dissipation rate equation is not adopted. The rotation effect in the present prediction is induced only from the rotational production and the absolute vorticity of the pressure-strain term in the full Reynolds stress equation.

In Fig. 1, the present redistribution tensor $\wp_{ij} (= kf_{ij})$ is compared with the KA-DNS [5] data for both rotation numbers Ro=0.15 and 0.5. In the case of Ro=0.5, the trend of kf_{ij} gives good results in comparison with the DNS data except for the near-wall region of the pressure side. However, the distribution of kf_{22} is underestimated in comparison with the DNS data at the core region of the channel. In the suction side which brings about a relaminarization, the profile of kf_{22} at Ro=0.15 is underestimated with the DNS data, whereas, at the pressure side, kf_{22} shows a better prediction for the redistribution.

Figure 2 shows the mean velocities non-dimensionalized by the bulk velocity for a non-rotational flow. The peak point of the mean velocity is shifted towards the suction side of the channel with increasing rotation number. The profiles show that the width of the linear slope region increases with the rotation number and the model predictions compare well with the DNS data. Figure 3 represents the profiles of Reynolds stress non-dimensionalized by a friction velocity. The streamwise normal stress u^+ corresponds to the DNS data in the suction side when rotating number is increasing. The wall-normal stress v^+ is gradually increased between y/2h=0.25 and 0.9, and is correctly reduced except for the suction side for Ro=0.15. At the distribution of shear stress uv^+ the positions of zero shear stress are shifted from the center of the channel towards the suction side when the rotation numbers are increased. Overall, the present model on the imposed system rotation shows a good agreement with the DNS data at higher rotation number.

Figure 4 displays the main velocity contours and the secondary flow vectors for the square straight rotating duct. The Coriolis term produces a considerable modification of the secondary flow near the

corners. Indeed, the rotating effect produces a secondary ascending flow that convects the fluid from the suction side (y=0) to the pressure side (y=1). The corresponding secondary descending flow is located at the corner near the pressure side where the axial velocity and the vertical component of the Coriolis force is smaller than in the center of the duct. At Ro=0.087, the cross-stream flows become asymmetric and the section perpendicular to the streamwise direction is constituted of four counter-rotations instead of eight vortices in the nonrotating square duct. The enlarged vortex near the top walls (y=1) decreases in size as the rotational number is increased. As shown in the main velocity contour figures, the Coriolis effects cause the contours of the main velocity to bulge towards the corners and shift the position of the maximum wall shear stress away from the center planes.

4. Conclusion

The present Reynolds stress model with the elliptic relaxation approach has been reported for the rotating flows. The present study was confined to high rotation numbers i.e. Ro up to 1.0 for Reynolds number 9500. In this range of rotation rates the observed effects of the imposed system rotation are primarily caused by the Coriolis force terms in the mean momentum equations. For the fully developed rotating flow, the correct response of the turbulence on the unstable side where the wall shear stress increased above the nonrotating levels and on the stable side where the reverse were observed. This model yields an asymmetric mean velocity and turbulence stresses in good concordance with the available results. The results presented above establish that the present elliptic relaxation RSM is a suitable approximation for the closure of the RANS equations in the three dimensional incompressible flows.

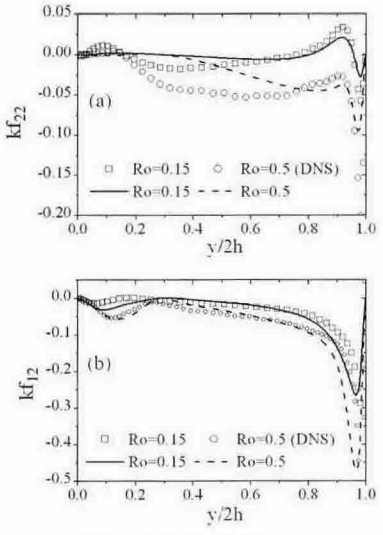

Figure 1. Redistribution tensors.

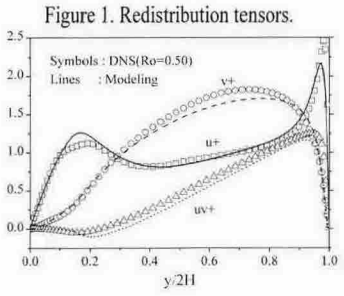

Figure 2. Reynolds stress at Ro=0.5.

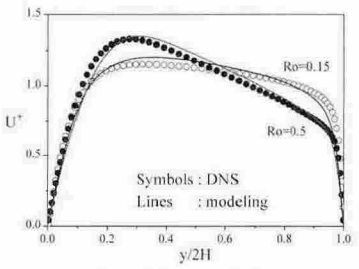

Figure 3. Mean velocity.

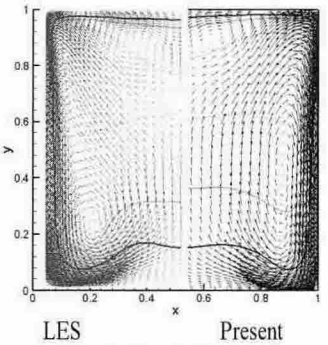

(a) Ro=0.087

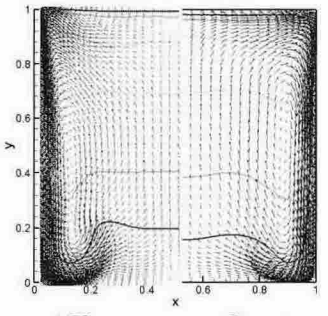

(b) Ro=0.12

Figure 4 Main velocity contour and secondary flow vectors

REFERENCES

[1] P. A. Durbin, "A Reynolds stress model for near-wall turbulence," J. Fluid Mech. **249,** 465 (1993).

[2] Wizman, D. Laurence, M. Kanniche, P. Durbin and A. Demuren, "Modelling near-wall effects in second-moment closures by elliptic relaxation," Int. J. Heat and Fluid Flow **17,** 255 (1996).

[3] B. A. Pettersson and H. I. Andersson, "Near-wall Reynolds-stress modelling in noninertial frames of reference," Fluid Dynamics Research **19,** 251 (1997).

[4] C. G. Speziale and T. B. Gatski, "Analysis and modelling of anisotropies in the dissipation rate of turbulence," J. Fluid Mech. **344,** 155 (1997).

[5] R. Kristoffersen and H. I. Andersson, "Direct simulations of low Reynolds number turbulent flow in a rotating channel," J. Fluid Mech. **256,** 163 (1993).